Corrosion behaviour of titanium in biofluids containing H_2O_2 studied by electrochemical impedance spectroscopy

C. Fonseca [a,b,*], M.A. Barbosa [a,b]

[a] *Laboratório de Biomateriais, Instituto de Engenharia Biomédica (INEB), Rua do Campo Alegre, 823, 4150-180 Porto, Portugal*
[b] *Faculdade de Engenharia, Departamento de Engenharia Metalurgica e de Materiais, Universidade do Porto, 4099 Porto, Portugal*

Abstract

This work aims at studying the electrochemical behaviour of titanium in the presence of an artificial biofluid containing H_2O_2, mimicking the situation, where the metal is implanted in the human body and hydrogen peroxide is generated by an inflammatory reaction. A phosphate buffered saline (PBS) solution and two PBS/H_2O_2 solutions containing 50 and 150 mM of H_2O_2 were used to simulate the body fluids. The behaviour of the metal was monitored as a function of time by electrochemical impedance spectroscopy (EIS) for three weeks. After one week, the PBS/H_2O_2 solutions were replaced by fresh PBS solutions in order to simulate the end of the inflammatory process and recovery of the system. All the experiments were carried out at a constant temperature of 37°C. From the simulation of the experimental EIS spectra, it was concluded that the corrosion resistance of titanium is strongly affected by the presence of H_2O_2 and when the peroxide is removed, the metal displays a sharp resistance increase. Furthermore, the oxides formed in H_2O_2 are rougher and display higher ionic conductivities than the oxides formed in the absence of peroxide. The study was complemented with potentiostatic experiments and scanning electron microscopy observation of the metal surfaces. © 2001 Elsevier Science Ltd. All rights reserved.

Keywords: Titanium; EIS; Corrosion; Biomaterials

* Corresponding author. Fax: +351-22-609-45-67.
 E-mail address: cfonseca@ibmc.pt (C. Fonseca).

1. Introduction

Titanium is nowadays one of the most common metallic materials for orthopaedic and dentistry applications. This is due to its excellent mechanical properties and corrosion resistance, which is ensured by a compact and chemically stable oxide film that spontaneously covers the metal surface. This film is about 5 nm thick, is amorphous or poorly crystalline and is composed of a slightly oxygen-deficient titanium oxide [1,2].

However, in spite of its excellent corrosion resistance when tested in vitro, important amounts of metal ions have been sometimes found in the tissues surrounding retrieved titanium implants [3–5]. Also, the thicknesses of the oxide films found in retrieved titanium implants were often much larger than the thicknesses reported for in vitro grown films [6,7]. It follows that the passivity of titanium in biological systems probably occurs under specific conditions, different from those observed in simple saline solutions.

A plausible explanation for the higher corrosion rates observed in vivo was proposed by Tengvall [8–10], and involves the generation of H_2O_2 during the inflammatory reaction triggered by the surgical process. It was showed that titanium is chemically attacked in the presence of H_2O_2, with the formation of a thick oxide layer on the metal surface and releasing of titanium ions to the solution. On the other hand, it has been demonstrated that titanium ions seem to have adverse effects on osteoblast function such as the production of specific bone proteins [11], to favour a thicker fibrous interface [12] or lead to the impairment of the immune response [13]. More recently Mu [14] has reported the in vitro effects of oxygen active species generated by rat macrophages, on the metal ion release from titanium. These effects could help to shed some light on the unexplained rejection of titanium implants in some cases.

In this work the electrochemical behaviour of titanium was followed in situ by electrochemical impedance spectroscopy (EIS) in a synthetic biofluid, the phosphate buffered saline (PBS) solution, to which H_2O_2 was added in small concentrations. After one week, the hydrogen peroxide solution was replaced by PBS and recovery of the system was followed for two weeks more. The EIS spectra were simulated according to a proposed equivalent electric circuit and the calculated parameters were analysed and discussed. Some complementary potentiostatic experiments and scanning electron microscopy (SEM) analysis of the sample surfaces were also carried out.

2. Experimental

Titanium electrodes were prepared from grade 2 commercial parity titanium rods with a diameter of 10 mm. The samples and electric contacts were sealed in an epoxy resin (Epofix, Struers), and the exposed surface was abraded with SiC paper of decreasing grain sizes down to grit #4000. Finally, the electrodes were sonicated in

ethanol (15 min) and distilled water (30 min), dried and the metal/resin interface was covered with a bees wax/colophony mixture (3:1) in order to avoid the crevice corrosion of the metal. The inflammatory conditions after implantation was simulated through the addition of H_2O_2 (30%, Merck) to the PBS solution (Sigma) to reach 50 and 150 mM peroxide concentrations. The pH of the final solutions was adjusted to 5.2, which is the pH during an inflammatory process, by adding a few drops of a 1M HCl solution. A PBS, H_2O_2 free solution was also used as a control. All the solutions were thermostatised at 37°C and the experiments were initiated by the immersion of freshly polished titanium electrodes. After one week, the PBS/H_2O_2 solutions were replaced by fresh PBS, which would correspond to the end of the inflammatory response, and the experiments were continued for two weeks more. The solutions were kept in a dark chamber in order to avoid the light assisted photodecomposition of H_2O_2. Electrochemical impedance spectra were acquired at intervals of one to two days using a Solartron 1250 frequency response analyser connected to a EG&G PAR 273 potentiostat and data acquisition was performed using the M388 program from EG&G PAR. The frequency ranged from 64 kHz to 2 mHz, and the amplitude of the a.c. signal was 7 mV. The three-electrode configuration was used with a SCE as the reference and a titanium electrode as the counter electrode (Pt cannot be used because it decomposes H_2O_2). The Boukamp [15] simulation software was used for the simulation of the EIS spectra. The SEM analysis was carried out in a Jeol JSM 6301F microscope.

3. Results

3.1. Assessment of the impedance data

The experimental impedance data was checked for the linearity and causality conditions through the calculation of Kronigs–Kramers (KK) transforms [16,17]. As is reported in the examples of Fig. 1 for the Ti–PBS interface, the KK relationships were verified in the whole frequency range within a 12% error, although a larger dispersion has been detected below, about 1 Hz. This was attributed to the high impedance displayed by the system for low frequencies. For most of the Ti–PBS/H_2O_2 interfaces, large shifts were observed for frequencies beyond, about 1–10 kHz, depending on the spectrum. Therefore, for the Ti–PBS/H_2O_2 interfaces only the frequencies falling in the 2 mHz to 1–10 kHz range were considered in the simulations. It is important to stress that the KK transforms provided us a justification for the bad fits in the high frequency ranges in these cases.

3.2. Equivalent electric circuit

Although the interaction mechanism between titanium and H_2O_2 has not been fully described, it is already known, after the works of Pan [18] and Tengvall [10], that corrosion of the metal occurs with the dissolution of titanium, formation of
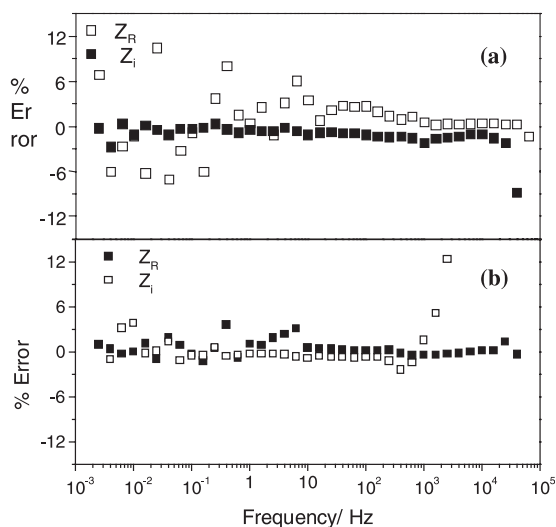
Fig. 1. Percentage difference between the real and imaginary parts of the experimental impedance and the data calculated from the KK transforms (a) Ti–PBS interface and (b) Ti–PBS/150 mM interface.

a titanium oxide film on the metal surface and Ti-catalysed decomposition of the peroxide. Based on this description of the system, the equivalent circuit depicted in Fig. 2 was proposed. The upper branch of the circuit corresponds to the electronic transfer at the interface, which was considered to be dominated by the electric properties of the oxide film. In the first simulation of the experimental spectra, a
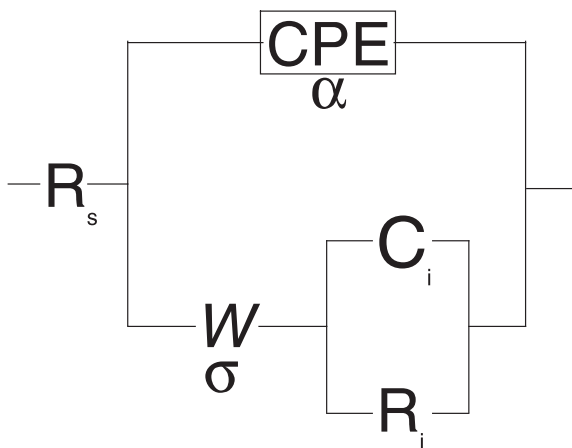

Fig. 2. Equivalent electric circuit used to simulate the Ti–PBS and Ti–PBS/H_2O_2 interfaces. R_s stands for the solution resistance, CPE stands for a constant phase element, W for a Warburg impedance inside the oxide film, R_i for the interfacial resistance and C_i for the interfacial capacitance. α and σ are the parameters representative of the corresponding circuit elements.

resistance was considered in parallel with the constant phase element (CPE), corresponding to the electronic resistance of the oxide, but the simulator always gave very high values for this parameter. Hence it was removed from the circuit. A CPE was used instead of a simple capacitance to take account of the porous/rough nature of the oxide as discussed below.

The lower branch corresponds to the Faradaic processes, namely releasing of titanium species to the electrolyte. W stands for the impedance due to the transport of oxygen and metal ions across the film which, according to Chao's model [19], is described by a Warburg impedance. The (C_i, R_i) elements represent, according with Armstrong [20], a dissolution process occurring at the film/electrolyte interface. C_i stands for the interfacial capacitance and R_i is the interfacial resistance or, which is the same, the corrosion resistance of the metal. The impedance behaviour of the Ti/ H_2O_2 interface was also studied by Pan [21], but used quite different experimental conditions (temperature, pH and immersion protocol) and a different circuit was also proposed to simulate the impedance spectra.

3.3. Discussion of the spectra

The circuit of Fig. 2 was used to simulate the experimental EIS spectra, allowing to obtain very good simulations (χ^2 values always of the order of 10^{-4} or inferior) for all the three solutions, namely PBS, PBS/50 mM H_2O_2 and PBS/150 mM H_2O_2. Two examples of the experimental and simulated spectra are reported in Fig. 3 as an example to notice, the strong evolution underwent by the Ti–PBS/H_2O_2 interface during the immersion period.
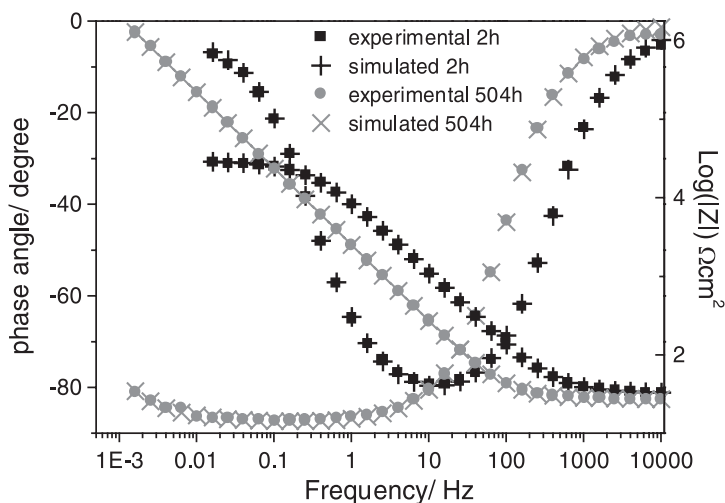

Fig. 3. Bode diagram for two examples of experimental and simulated EIS spectra taken at different times for a titanium sample immersed in PBS with a 150 mM H_2O_2 concentration. $T = 37°C$.
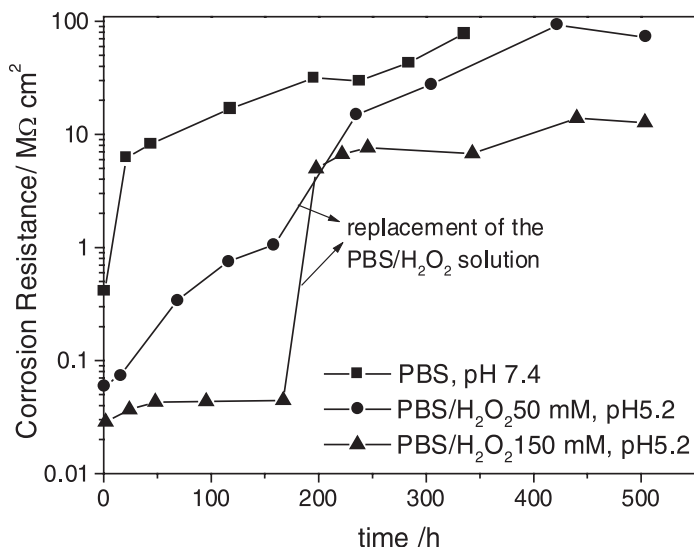
Fig. 4. Corrosion resistance vs time for titanium samples immersed in different PBS solutions, calculated from the simulations of the EIS spectra. The PBS/H$_2$O$_2$ solutions were replaced by fresh PBS solutions after about 180 h. $T = 37$°C.

3.4. Evolution of R_i vs time

In Fig. 4 the R_i vs time calculated from the simulations for the three studied situations are reported. The PBS immersed sample displays the higher corrosion resistances, as it was expected, due to the high corrosion resistance of titanium in water saline solutions. The relatively low values observed for the first immersion times are attributed to the use of a freshly polished sample. It is apparent that the corrosion resistance of titanium is strongly affected by the presence and concentration of H$_2$O$_2$, decreasing up to about 300 times for the more concentrated H$_2$O$_2$ solution. However, when the PBS/H$_2$O$_2$ solutions are replaced by fresh PBS, R_i sharply increases and for the case of the less concentrated H$_2$O$_2$ solution, it even reaches the values of the control sample after two weeks.

3.5. Evolution of α vs time

This coefficient has been first introduced by Cole [22] for the study of dielectric relaxation phenomena in solids, in order to take account of the depressed semicircles in the plots of the real vs imaginary parts of the dielectric constant. Later, the depressed semicircles were also observed in the EIS spectra when the Nyquist representation was adopted. For the electrochemical interfaces, the physical meaning of this factor has been attributed to the surface roughness [23], the presence of a porous corrosion product layer [24,25], or the heterogeneous nature of the surface [16].
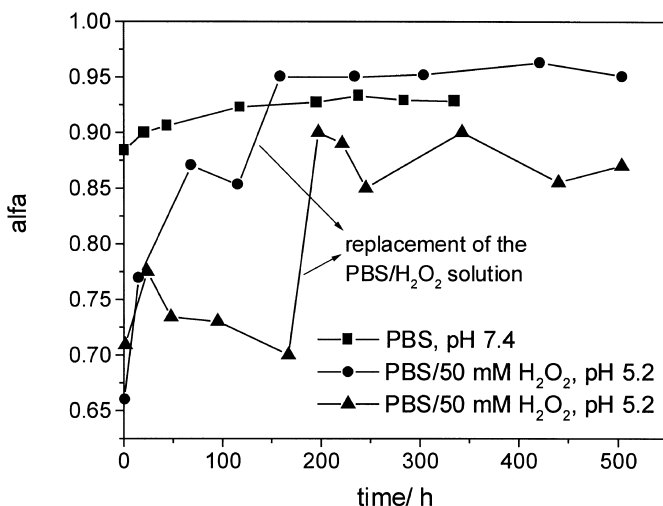
Fig. 5. Evolution of the α parameter of the CPE, calculated from the EIS simulated spectra for the three PBS solutions. $T = 37$°C.

The plots of α vs time for the three interfaces are reported in Fig. 5. For the oxide formed in the PBS solution, α increases with time and stabilises after about one week, while for the H_2O_2 formed oxides, α is noticeably lower and the higher the peroxide concentration the lower the value. After the replacement of the H_2O_2 solutions, α increases and in the case of the lower peroxide concentration, it even reaches the values found for the PBS grown oxides.

3.6. Evolution of the Warburg impedance with time

This term takes account of the impedance related with the ionic transport through the oxide. It is represented by σ and depends on the concentration, charge and diffusion coefficients of the metal and oxygen ions [19]. The higher the σ, the higher the blocking character of the oxide. The plots for this parameter are reported in Fig. 6. It can be concluded that the PBS grown oxide display the highest σ values. The oxides grown in the peroxide solutions have a significantly lower blocking character, what can be explained by a more defective and/or porous nature of the oxides in these cases. The higher the peroxide concentration, the lower the σ and the removal of the H_2O_2 does not seem to affect this parameter.

3.7. Open circuit potential vs time curves

The plots for the open circuit potential vs time are reported in Fig. 7(a). The same trend is followed by the three curves up to about 180 h immersion, the point, where the PBS/H_2O_2 solutions were replaced by fresh PBS. Beyond this point, the open
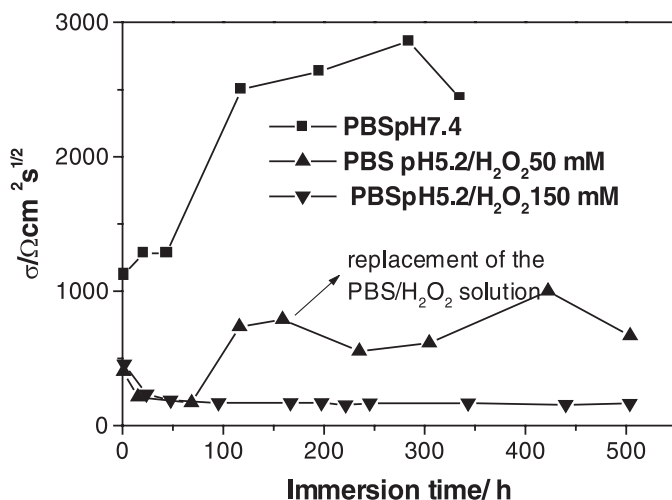
Fig. 6. Evolution of the Warburg parameter, σ, calculated from the simulation of the EIS spectra for the three PBS solutions. $T = 37°C$.

circuit potentials tend to a common value. According to Tengvall studies [9,10], the higher potentials displayed in the H_2O_2 solutions can be related with the adsorption to the oxide of intermediates with a strong oxidising character, such as TiO_2, HO_2 or HO. Therefore, the elimination of such species from the metal surface will be responsible for the potential drop seen in Fig. 7(a) when the solutions are replaced. It is interesting to notice that the highest potentials are attained for less concentrated peroxide solution. No plausible explanation was found for this behaviour.

If a time logarithmic scale is adopted for the plots, a linear behaviour is observed for the three plots, Fig. 7(b), as previewed by Kader's model [26,27] for the open circuit thickening of a metal oxide film in aqueous solution. The thickening rates were calculated, in accordance with the model, from the slopes of the lines and are reported in Table 1. It can be concluded that the thickening rates for the PBS and PBS/50 mM H_2O_2 are very similar. The lower value found for the PBS/150 mM H_2O_2 solution may be due to a higher dissolution rate of the oxide in this solution. Although the growing rates for the PBS/H_2O_2 solutions could not be confirmed, the value estimated for the PBS solution is in good agreement with the one reported by Hanawa [28]. This author performed direct XPS measurements of the thickness of titanium oxides grown on titanium immersed for several periods in HBSS (a biofluid similar to PBS).

3.8. SEM analysis

The samples surfaces were observed by SEM after a seven days immersion period in each of the solutions, Fig. 8(a)–(c). A roughness increase is apparent from the
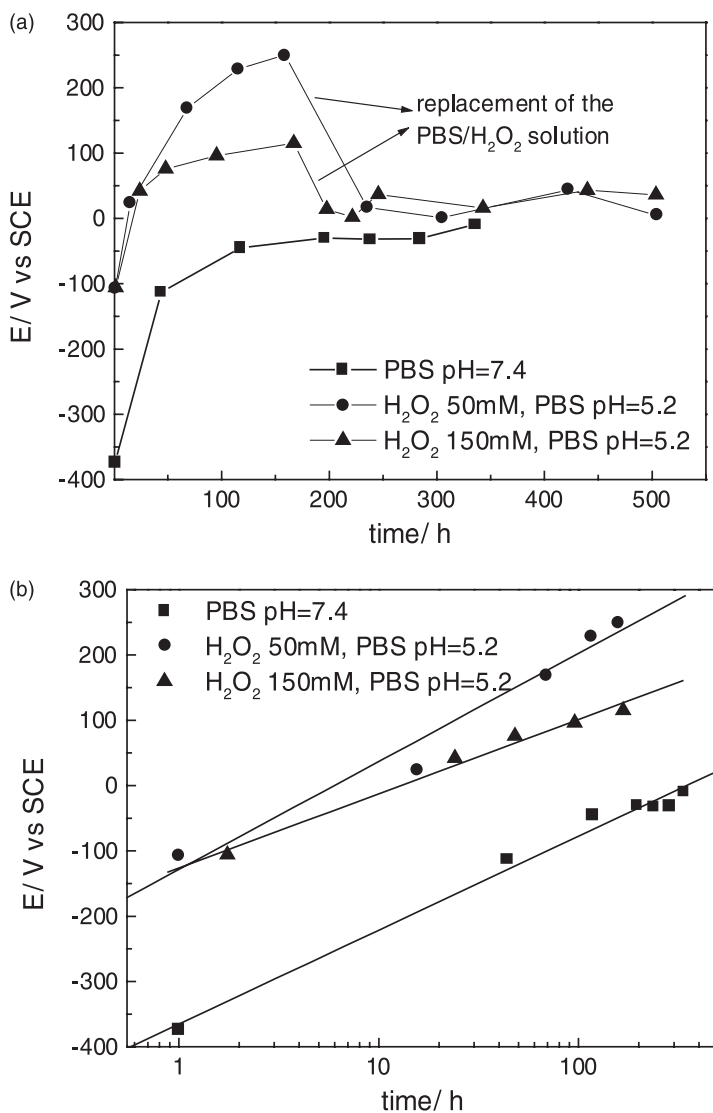
Fig. 7. (a) Open circuit potential vs time for titanium samples immersed in the three PBS solutions, $T = 37°C$ and (b) same plots represented in a logarithmic time scale for the period before the replacement of the PBS/H_2O_2 solutions.

Table 1
Values of the thickening rates estimated from the slopes of the plots of Fig. 7(b)

Solution	Thickening rate nm per unit decade of time (h)
PBS	2.4
PBS/50 mM H_2O_2	2.8
PBS/150 mM H_2O_2	1.9

PBS sample to the PBS/50 mM H_2O_2 sample and especially from this one to the PBS/150 mM sample. In this case, the oxide clearly shows a porous structure and the photo show two differently attacked grains, what was often observed for this surface, Fig. 8(c). Pitting attack can also be observed in both the PBS/H_2O_2 treated samples.
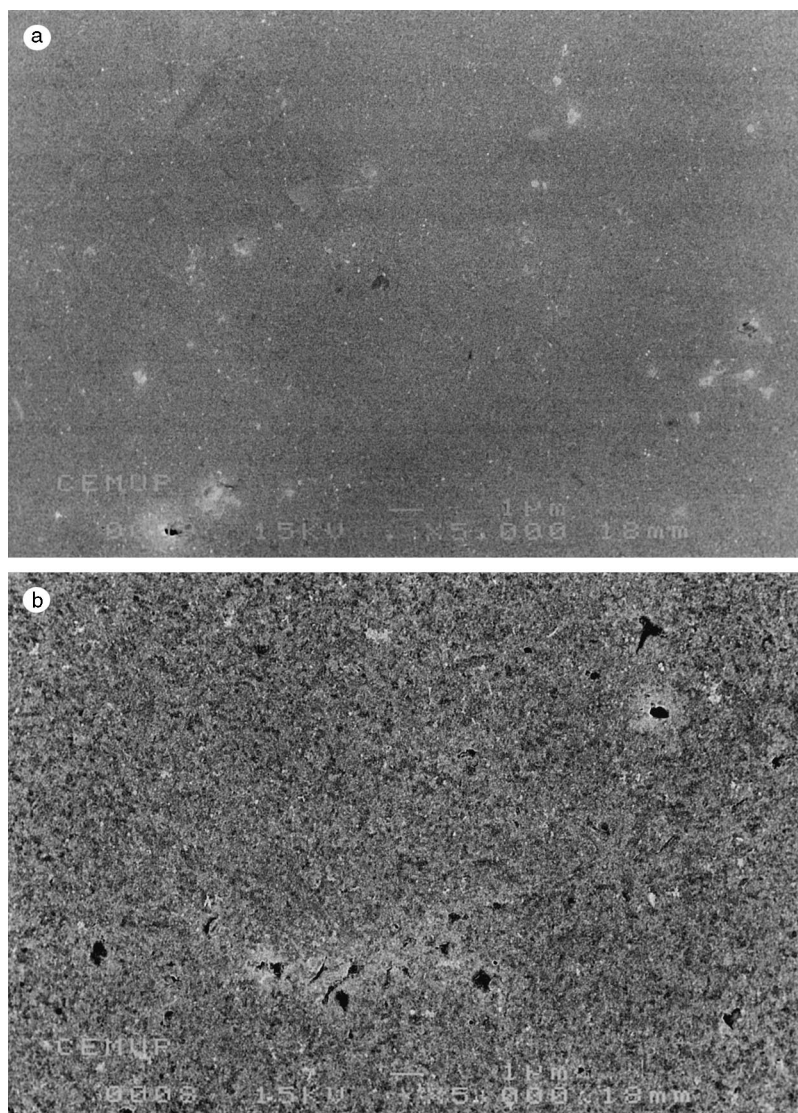

Fig. 8. Scanning electron micrographs of titanium samples after a seven days immersion period in (a) PBS, (b) PBS/50 mM H_2O_2 and (c) PBS/150 mM H_2O_2.
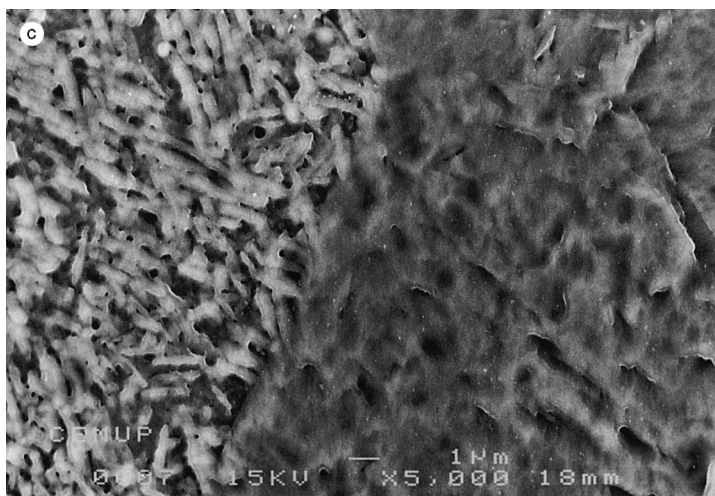
Fig. 8 (*continued*)

4. Discussion

In a perspective of the application of titanium as a bio implant, the plots of Fig. 4 contain the most useful information calculated from the simulations. For the case of the PBS solution, the increase of R_i is due to the thickening of the oxide film and probably also to the improvement of its insulating properties with ageing under the influence of the high interfacial electrostatic field (e.g. through oxidation of the remaining Ti(III) to Ti(IV) or the elimination of point defects). This is in line with the time increase of the Warburg impedance, Fig. 6, or even the increase of the α parameter, Fig. 5, that can also be explained in terms of the formation of a more compact and insulating oxide.

When titanium is brought into contact with H_2O_2 two phenomena will take place at the metal interface, (i) the Ti-catalysed decomposition of hydrogen peroxide and (ii) the corrosion of the metal, which will involve the metal dissolution into the electrolyte and the formation of a titanium oxide. This oxide is far thicker than the one obtained by simple immersion of the metal in saline solutions for similar periods [18] and is composed of two layers: an outer layer highly porous and hydroxylated and an inner layer, much thinner and with an insulating character [18,29]. This layer will be responsible for the potential drop in the oxide, thus the thickening rates calculated from the open circuit potentials vs time plots (Fig. 7(b) and Table 1) must refer to that part of the oxide only. Since the thickening rates are very similar for both the PBS and PBS/H_2O_2 layers, it can be concluded that the thickness of the inner PBS/H_2O_2 layers must be of the order of only a few nanometers. Hanawa [30] reported a 6 nm value for the thickness of a two weeks grown oxide. Once the total thickness of the H_2O_2 formed oxides is of the order of 40 nm as it was estimated from their interference colours, the hydroxylated layer should represent about 90% of the film.

Although the mechanisms of titanium corrosion in H_2O_2 are not yet fully understood some intermediary species, mainly of anionic character, have been postulated or already identified [8,9]. We think that a high concentration of these anionic species must exist at the oxide/electrolyte interface, creating a strong electrostatic field in the oxide that will accelerate the titanium oxidation and the ionic migration towards the oxide/electrolyte interface. That could explain the lower corrosion resistance of titanium when peroxide is present. Therefore, the sharp rise of R_i when PBS replaces the PBS/H_2O_2 solution, Fig. 4, should be related with the elimination of these adsorbed anionic charges from the oxide surface.

Both the α parameter and the Warburg diffusion coefficient are significantly lower for the PBS/H_2O_2 grown oxides than for the PBS grown layers. While the lower Warburg coefficients indicate less insulating oxides formed in this cases, the α values should be related with the formation of porous and rough oxides [31,32], or even to the chemical attack of the layers, since α increases when H_2O_2 is removed. It is also possible that the CPE in these cases takes account of the undetermined circuit elements related with the chemical/physical processes occurring at the interface. These effects are shown to increase for increasing peroxide concentrations and the rough and porous nature of the layers was confirmed through SEM observation of the samples surfaces for the three situations, Fig. 8(a)–(c).

5. Conclusions

The electrochemical behaviour of titanium in PBS/H_2O_2 electrolytes was studied by EIS. The simulation of the experimental spectra allowed monitoring the corrosion resistance of the system in the three analysed solutions, PBS, PBS/50 mM H_2O_2 and PBS/150 mM H_2O_2 as a function of the immersion time. The corrosion resistance displays its highest values for the PBS immersed sample and is significantly lower for the PBS/H_2O_2 solutions, especially for the more concentrated one. For this situation R_i is about 300 times lower than for the control PBS solution. An increase of R_i is noticed for both peroxide solutions when the H_2O_2 is removed. Two other parameters related with the oxide film were also calculated from the EIS fits, namely the Warburg diffusion coefficient and the α parameter from the CPE. These parameters indicated that the oxides formed in the H_2O_2 electrolytes are rougher and less blocking than the oxides formed in the absence of the oxidant.

It can be concluded that the equivalent electric circuit proposed in this work provide a reliable description of the corroding interface, owing to the quality of the fits and the coherence of the results obtained from the calculated parameters.

References

[1] lA. Hugot-Le-Goff, Thin Solid Films 142 (1986) 193.

[2] P. Pascal (Ed.), Nouveau Traité de Chimie Minérale, vol. 14, Masson & Cie, Paris, 1963.

[3] P.G. Laing, A.B. Ferguson, E.S. Hodge, J. Biomed. Mater. Res. 1 (1967) 135.

[4] L.D. Dorr, R. Bloebaum, J. Emmanual, R. Meldrum, Clin. Orthop. 261 (1990) 82.

[5] G. Meachim, D.F. Williams, J. Biomed. Mat. Res. 7 (1973) 555.

[6] J.E. Sundgren, P. Bodö, I. Lundström, J. Colloid Interf. Sci. 10 (1986) 9.

[7] D. McQueen, J.E. Sundgren, B. Ivarsson, I. Lundström, B. Ekenstam, A. Svensson, P.I. Brånemark, T. Albrektsson, Auger electron spectroscopic studies of titanium implants, in: A.J.C. Lee, T. Albrektsson, P.I. Brånemark (Eds.), Clinical Applications of Biomaterials, Wiley, 1982, p. 179.

[8] P. Tengvall, H. Elwing, L. Sjöqvist, I. Lundström, L.M. Bjursten, Biomaterials 10 (1989) 118.

[9] P. Tengvall, I. Lundström, Clinical Mater. 9 (1992) 115.

[10] P. Tengvall, H. Elwing, I. Lundström, J. Colloid Interf. Sci. 130 (1989) 405.

[11] Z.L. Sun, J.C. Wataha, C.T. Hanks, J. Biomed. Mater. Res. 34 (1997) 29.

[12] E. Schepers, M. Clercq, P. Ducheyne, Tissue response to a bioactive glass–metal interface, in: C.D. Putter (Ed.), Implant Materials in Biofunction, Elsevier, Amsterdam, 1987, p. 79.

[13] J.Y. Wang, D.T. Tsukayama, B.H. Wicklund, R.B. Gustilo, J. Biomed. Mater. Res 32 (1996) 655.

[14] Y. Mu, T. Kobayashi, M. Sumita, A. Yamamoto, T. Hanawa, J. Biomed. Mat. Res. 49 (2000) 238.

[15] B. Boukamp, Equivalent Circuit, User's Manual, 2nd revised edition, Un. Twente Enschede, The Netherlands, 1989.

[16] J.R. MacDonald, W.B. Johnson, (Eds.), Impedance Spectroscopy, John Wiley, New York, 1987, pp. 154–156.

[17] D.D. MacDonald, M. Urquidi-MacDonald, J. Electrochem. Soc. 133 (1985) 2018.

[18] J. Pan, D. Thierry, C. Leygraf, J. Biomed. Mater. Res. 28 (1994) 113.

[19] C.Y. Chao, L.F. Lin, D.D. MacDonald, J. Electrochem. Soc. 129 (1982) 1874.

[20] R.D. Armstrong, K. Edmondson, Electrochim. Acta 18 (1973) 937.

[21] J. Pan, D. Thierry, C. Leygraf, Electrochim. Acta 41 (1996) 1143.

[22] K.S. Cole, R.H. Cole, J. Chem. Phys. 9 (1941) 341.

[23] U. Rammlet, G. Reinhard, Corros. Sci. 27 (1987) 373.

[24] F. Mansfeld, H. Shih, H. Greene, C.H. Tsai, Analysis of EIS-data for common corrosion processes, Int. Symp. on Electrochem. Imp. Analysis and Interpretation, ASTM STP, San Diego, 1991.

[25] J.R. Park, D.D. MacDonald, Corros. Sci. 23 (1983) 295.

[26] J.M.E. Kader, A.M.E. Din, Br. Corros. J. 14 (1979) 40.

[27] J.M.E. Kader, F.M.E. Wahab, H.A.E. Shayeb, M.G. Khedr, Br. Corros. J. 16 (1981) 111.

[28] T. Hanawa, M. Ota, Biomaterials 12 (1991) 767.

[29] J. Pan, D. Thierry, C. Leygraf, J. Biomed. Mater. Res. 30 (1996) 393.

[30] T. Hanawa, M. Ota, Appl. Surf. Sci. 55 (1992) 269.

[31] A. Le Mehaute, J. Stat. Phys. 36 (1984) 665.

[32] De Levie, Electrochemical response of porous and rough electrodes, in: P. Delahay (Ed.), Advances in Electrochemistry and Electrochemical Engineering, vol. 6, Interscience, NY.